Supporting Information

Chauveau et al. 10.1073/pnas.0910074107

SI Materials and Methods

Cells and Constructs. Peripheral blood NK cells were isolated by negative selection from healthy donor buffy coat using magnetic beads (NK cell isolation kit; Miltenyi Biotec) and cultured as described previously (1). Where indicated, freshly isolated cells were stimulated for 24 h with either 150 U·mL^{-1} human recombinant IL-2 (Roche), 10 ng·mL^{-1} IL-12, 10 ng·mL^{-1} IL-15, or 100 ng·mL^{-1} IL-18 (all from Prepro Tech, Inc.). Purity and activation of NK cells were confirmed by flow cytometry using FITC-labeled anti-CD3 (clone HIT3a), Allophycocyanin (APC)-labeled anti-CD56 (clone B159), and FITC-labeled anti-CD69 (clone FN50) mAb (all from BD Biosciences). NKL, P815, THP-1, 221, Daudi/MICA (2), and transfectants were cultured in RPMI, 10% (vol/vol) FBS, 2 mM L-glutamine, 1 mM sodium pyruvate, nonessential amino acids, 50 U·mL^{-1} penicillin, and 50 μg·mL^{-1} streptomycin (Invitrogen). NKL was supplemented with 100 U·mL^{-1} human recombinant IL-2 (Roche). P815 was transfected with pcDNA3.1-MICA-YFP (3) or pEYFP-Mem (Clontech) by electroporation (Biorad) and selected with 1.6 mg·mL^{-1} geneticin. Plasmids encoding DAP-10-GFP and Vav-1-GFP were generated by PCR and inserted as BglII/Not1 or Bcl1/Not1 fragments in the PINCO vector (kindly provided by M. Caligiuri, Ohio State University, Columbus, OH). DAP10(Y85F)-GFP was generated by mutagenesis PCR (Quickchange Site-directed mutagenesis kit; Stratagene) using the following primers: forward 5′-GCC CAA GAT GGC AAA GTC TTC ATC AAC ATG CCA GGC AGG-3′ and reverse 5′-CCT GCC TGG CAT GTT GAT GAA GAC TTT GCC ATC TTG GGC-3′, as previously described (4). The amphotropic packaging cell line Phoenix was transfected with PINCO-DAP10-GFP, PINCO-DAP10(Y85F)-GFP, or PINCO-Vav-1-GFP plasmid using Lipofectamin LTX (Invitrogen). Viral supernatant was collected 24 and 48 h after transfection. For infection, 5×10^5 mL^{-1} NKL cells were subjected to three sequential centrifugations (45 min, 725 × *g*) in the presence of the viral supernatant. Cells expressing GFP were enriched by flow cytometry 1 week later (5). NK cell cytotoxicity against different target cells was assessed in standard ^{35}S-Met release assays performed in triplicate.

Estimation of the Number of MICA Molecules. P815/MICA-YFP was cloned by limiting dilution, and surface expression of MICA was analyzed by flow cytometry using an APC-conjugated anti-MICA mAb (clone 159227; R&D Systems), which correlated with YFP fluorescence (R^2 = 0.9). The number of MICA proteins expressed by each clone was determined using a standard bead-based assay (Quantum Simply Cellular; Bangs Laboratories and FlowJo software; Tree Star, Inc.) (1). Clones generated expressed ∼200–430,000 molecules at their surface.

Estimation of the Amount of MICA at Nanotube Junctions. The total YFP fluorescence of each individual cell was quantified from the sum of fluorescence in a stack of optical slices (ImageJ software; National Institutes of Health). The distribution of fluorescence in cells that were imaged was then plotted and compared with the distribution of MICA determined by flow cytometry for the same cell population. In this manner, the fluorescence from an individual cell was positioned within the distribution of fluorescence across the population of cells. Separately, the mean number of MICA proteins expressed in the population of cells was quantified by flow cytometry using beads with known numbers of antibody binding sites. This allowed the position of a cell within the distribution of fluorescence to be translated to a specific number of MICA proteins being expressed by that cell. The area of the cell was then measured to estimate the density of surface MICA on an individual cell. The fold increase in fluorescence at the nanotube junction was then measured to calculate the density of proteins at a nanotube junction. The size of the nanotube junction was estimated from fluorescence images and used to estimate the number of MICA proteins at the nanotube junction.

Fixation, Immunostaining, and mAb-Blocking Experiments. NKL cells were incubated with target cells for 45 min, fixed, and quenched as previously described (6). Cells were stained with anti-α-tubulin mAb (clone DM 1A; Sigma), anti-perforin (clone δG9; BD Biosciences), or anti-phosphotyrosine mAb (clone 4G10; Upstate), followed by cy5-conjugated AffiniPure goat anti-mouse IgG antibody (Jackson ImmunoResearch) at room temperature for 45 min. F-actin was stained using Alexa-633-conjugated phalloidin (Molecular Probes). For mAb-blocking experiments, NKL cells were preincubated for 30 min in medium containing either 5 μg·mL^{-1} isotype-matched control mAb (IgG1; R&D Systems) or 5 μg·mL^{-1} anti-NKG2D mAb (R&D Systems) and then incubated for 1 h with P815/MICA-YFP in the presence of the mAb.

Manganese Stimulation. NKL cells and P815/ICAM-1-GFP cells were washed with buffer containing 10 mM Hepes, 140 mM NaCl, and 1 g·L^{-1} glucose and were incubated for 1 h in the same medium with or without 1 mM $MnCl_2$ [as previously described (7)].

Imaging in a 3D Environment. For imaging in a 3D matrix, 10^5 NKL cells labeled with DiD were mixed with 10^5 P815/MICA-YFP in BD Matrigel Basement Membrane Matrix (BD Biosciences); diluted 1:4 with cell culture media supplemented with IL-2; and imaged at 37 °C, 5% (vol/vol) CO_2 by resonance scanning laser scanning confocal microscopy using a 20× dry objective (N.A. = 0.5).

Quantification of Cell Polarity. Target cells were considered polarized when the ratio between the largest and smallest cell diameters was greater than 1.2. The orientation of polarized cells (i.e., location of the leading edge and uropod) was assessed visually (examples shown in Fig. S7).

Removing the Nanotube Using a Micromanipulator. For removing the nanotube, a micromanipulator (Injectman NI2, V1.10; Eppendorf) equipped with a sterile needle with an external diameter of 7 μm (TransferTips-F; ICSI) was used either to move the NK cell away from the target cell or to poke the nanotube itself directly. During removal of the nanotube, cells were imaged every 1 sec in the x-y plane. Target cells were then followed by imaging by collecting a z-stack every 2 min for the next 150 min in the presence of the DNA dye Sytox-blue.

Statistical Analysis. All data were tested (GraphPad software; Prism) for their normality using a D'Agostino and Pearson omnibus normality test. In Figs. 1 *C* and *D*, 3 *A, B, E*, and *G*, and 6 *C* and *H* and Figs. S1 *D* and *E*, S4*C*, and S8, one-way ANOVA tests, followed by a series of *t* tests, were used. For Fig. 6I, because the distribution was not normal, Kruskal–Wallis tests were used, followed by a series of Mann–Whitney *U* tests. In Figs. 2 *B* and *C*, 3 *C* and *F*, 4 *B* and *C*, 5 *B*, *C*, and *F* and Figs. S2 *D* and *E* and S6*D*, Mann–Whitney *U* tests were used. In Fig. 6*B*, a *t* test was used. Mean values are shown, and error bars are shown as SEM unless stated otherwise.

1. Almeida CR, Davis DM (2006) Segregation of HLA-C from ICAM-1 at NK cell immune synapses is controlled by its cell surface density. *J Immunol* 177:6904–6910.
2. Eleme K, et al. (2004) Cell surface organization of stress-inducible proteins ULBP and MICA that stimulate human NK cells and T cells via NKG2D. *J Exp Med* 199:1005–1010.
3. McCann FE, Eissmann P, Onfelt B, Leung R, Davis DM (2007) The activating NKG2D ligand MHC class I-related chain A transfers from target cells to NK cells in a manner that allows functional consequences. *J Immunol* 178:3418–3426.
4. Billadeau DD, Upshaw JL, Schoon RA, Dick CJ, Leibson PJ (2003) NKG2D-DAP10 triggers human NK cell-mediated killing via a Syk-independent regulatory pathway. *Nat Immunol* 4:557–564.
5. Grignani F, et al. (1998) High-efficiency gene transfer and selection of human hematopoietic progenitor cells with a hybrid EBV/retroviral vector expressing the green fluorescence protein. *Cancer Res* 58:14–19.
6. Sowinski S, et al. (2008) Membrane nanotubes physically connect T cells over long distances presenting a novel route for HIV-1 transmission. *Nat Cell Biol* 10: 211–219.
7. Dransfield I, Cabañas C, Craig A, Hogg N (1992) Divalent cation regulation of the function of the leukocyte integrin LFA-1. *J Cell Biol* 116:219–226.

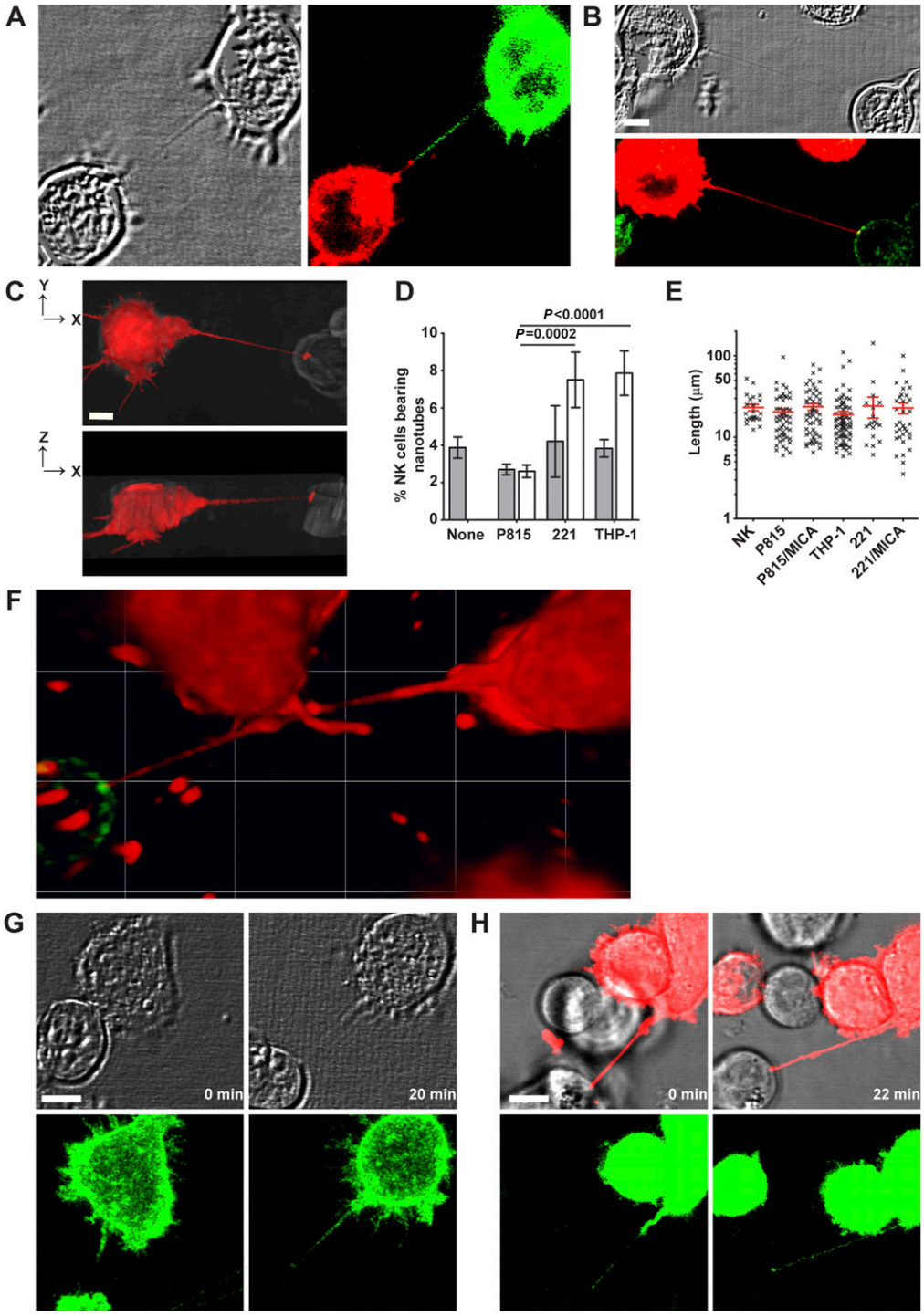

Fig. S1. Human NK cells readily form membrane nanotubes. NKL cells labeled with DiD (red) readily formed nanotubes with other NKL cells labeled with DiO (green, $n > 200$) (*A*) or with P815/MICA-YFP (green, $n > 500$) (*B*). (*C*) Two views at different orientations of a reconstructed nanotube between NKL cells stained with DiD (red) and P815/MICA show that nanotubes lie above the substratum. For orientation, three axes (x, y, z) are indicated. (*D*) After 45 min of coculture, the frequency of nanotubes formed by NKL was assessed for cells incubated alone (none) or in the presence of different target cells as indicated ($n > 1{,}500$ cells). Bars show the frequency of nanotubes between NK cells (shaded) and the frequency of nanotubes connecting NK cells to target cells (white). (*E*) Length of nanotubes formed between NKL and different target cells was assessed and could sometimes reach over 100 μm ($n > 260$). (*F*) Membrane nanotubes form between NKL cells stained with DiD (red) and P815/MICA-YFP (green) in a 3D extracellular matrix ($n = 50$, scale unit = 25 μm). (*G*) Time-lapse images showing NKL/mem-YFP (green) and P815/MICA, revealing the nanotube junction ($n = 10$). (*H*) Representative example of time-lapse microscopy of NKL transfected to express cytoplasmic GFP (green) and labeled with DiD (red) connected to a P815/MICA target cell ($n = 5$). (Scale bars: 10 μm.)

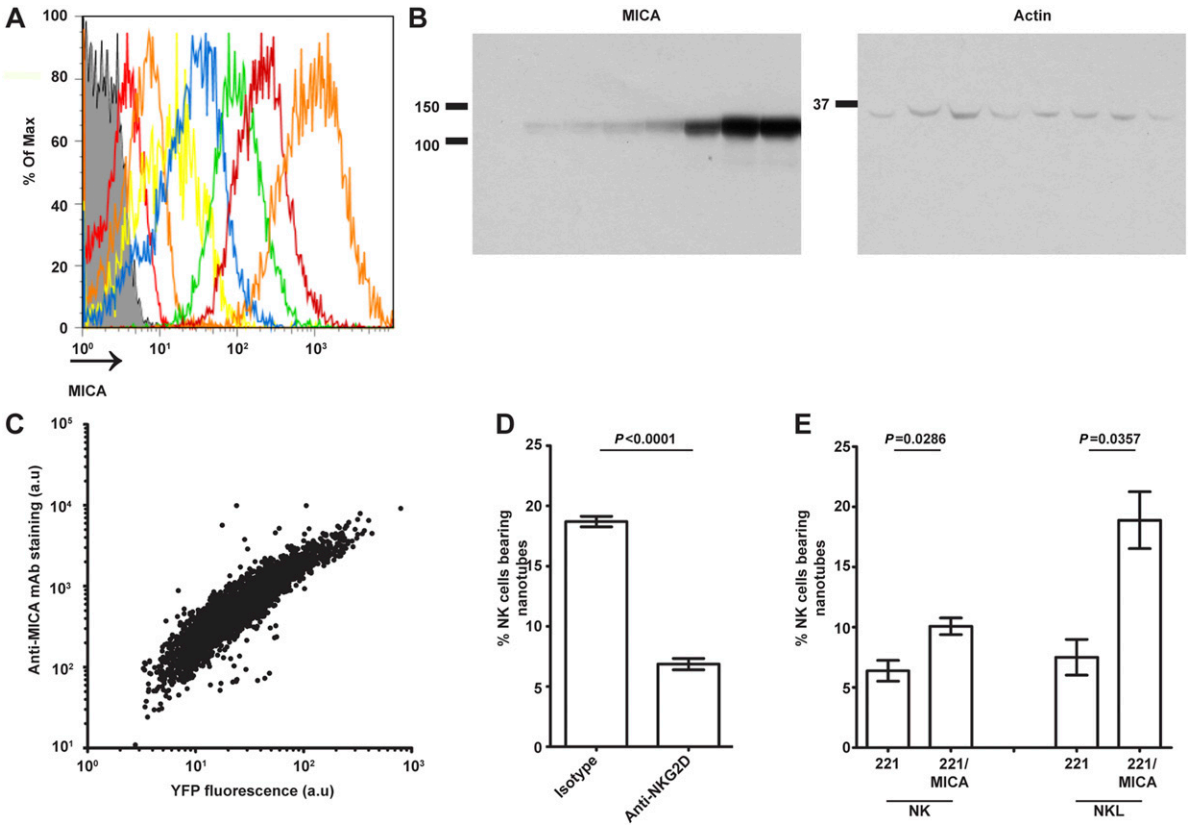

Fig. S2. Characterization of P815 cells expressing various levels of MICA proteins. (*A*) Level of MICA staining, detected by flow cytometry, on P815 cells transfected to express MICA proteins and selected for different levels of expression. (*B*) Total level of MICA expressed in the different lines was also confirmed by Western blotting with an anti-MICA mAb. Western blots for actin indicate similar loading in different lanes of the gel. (*C*) YFP fluorescence is plotted against the surface staining of cells with anti-MICA mAb conjugated to APC. This confirms that total MICA expression correlates to surface levels of MICA (Spearman $r = 0.9154$, $P < 0.0001$). (*D*) Frequency at which NKL formed nanotubes with P815 transfectants expressing high levels of MICA in the presence of anti-NKG2D mAb or an isotype-matched mAb ($n > 1{,}000$). (*E*) Frequency at which NK cells formed nanotubes was assessed for cocultures of primary NK cells (NK) or NKL cells (NKL) and untransfected 221 or transfectants of 221 expressing MICA-YFP (221/MICA, $n > 1{,}500$).

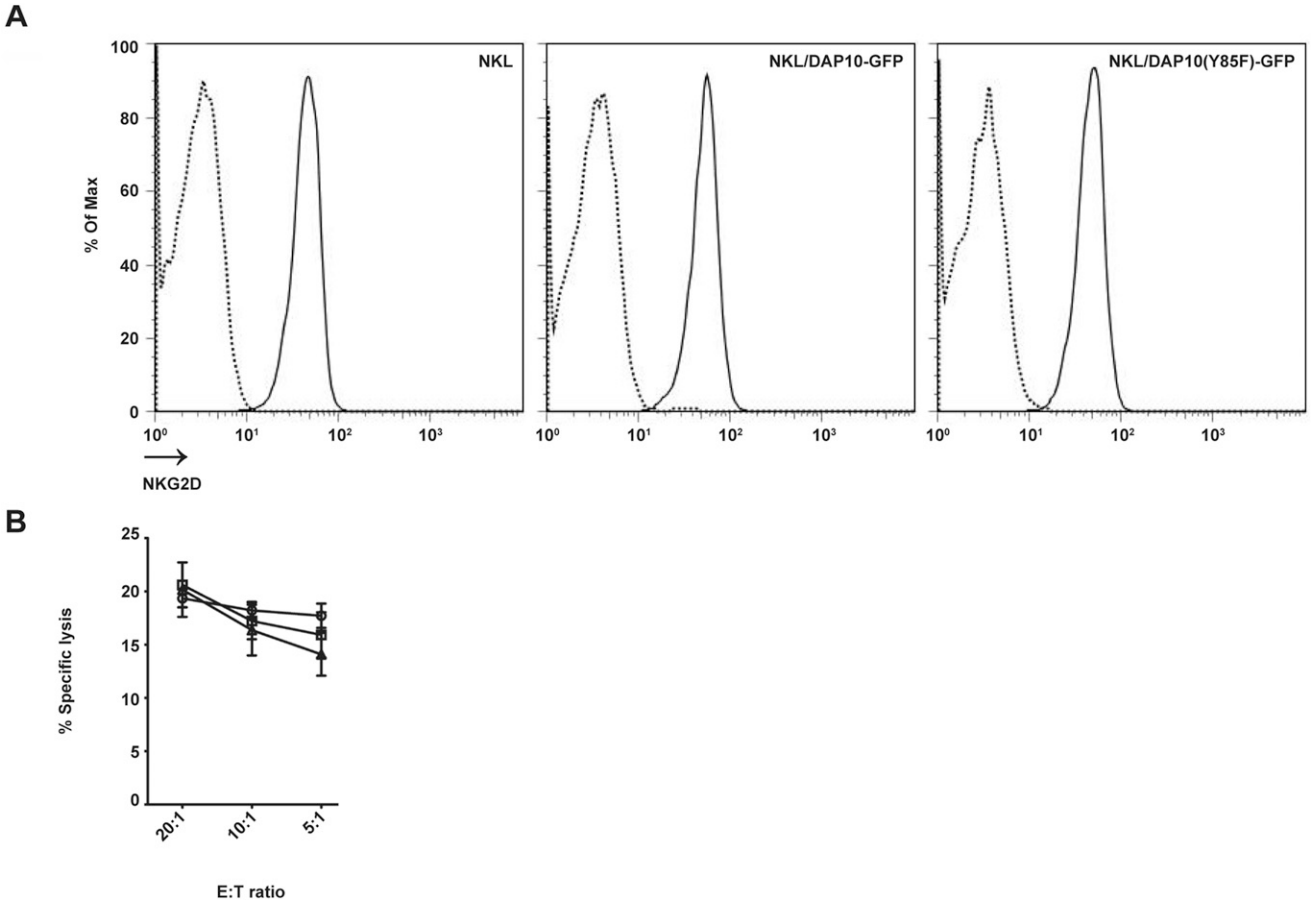

Fig. S3. (*A*) Expression of NKG2D at the surface of untransfected NKL or NKL transfected to express either WT DAP10-GFP or DAP10(Y85F)-GFP. Panels compare staining by anti-NKG2D mAb (solid line) with isotype-matched control mAb staining on the same cells (dashed line). (*B*) Percent specific lysis of 221 by untransfected NKL (□), NKL/DAP10-GFP (△), or NKL-DAP10(Y85F)-GFP (○) at three E/T ratios.

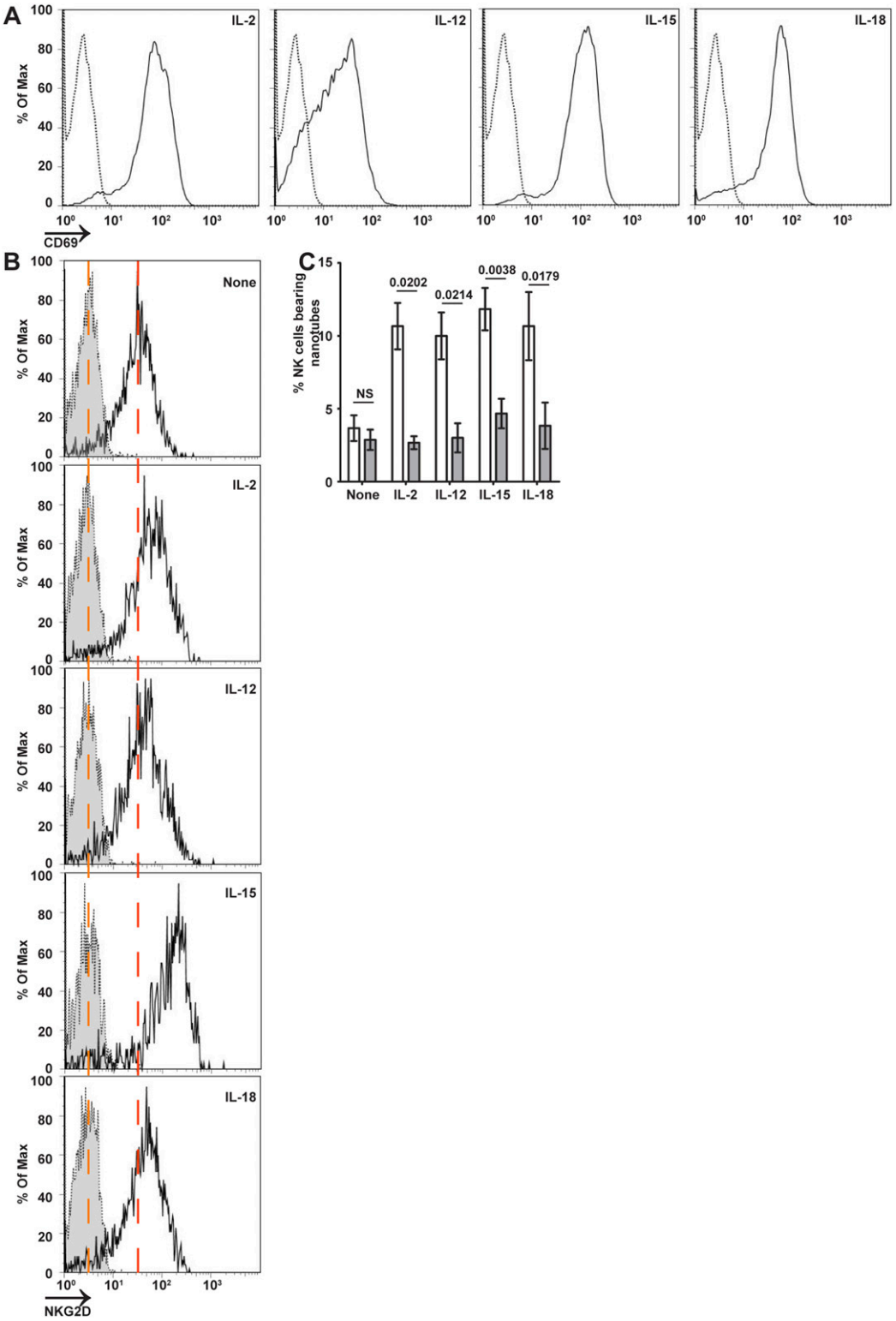

Fig. S4. (*A*) Activation of freshly isolated NK cells with cytokines. After 24 h of stimulation with IL-2, IL-12, IL-15, and IL-18, primary NK cells were stained for CD69 and analyzed by flow cytometry. Staining is compared by anti-CD69 mAb on stimulated NK cells (solid line) or unstimulated cells (dashed line). (*B*) Either without stimulation or after 24 h of stimulation with IL-2, IL-12, IL-15, and IL-18, primary NK cells were stained with anti-NKG2D mAb (black line) or an isotype-matched control mAb (filled histogram) and analyzed by flow cytometry. (*C*) Freshly isolated human NK cells were incubated with different cytokines as indicated and assessed for the frequency at which they made nanotubes with P815/MICA-YFP in the presence of anti-NKG2D mAb (filled bars) or an isotype-matched control mAb (white bars, $n > 900$).

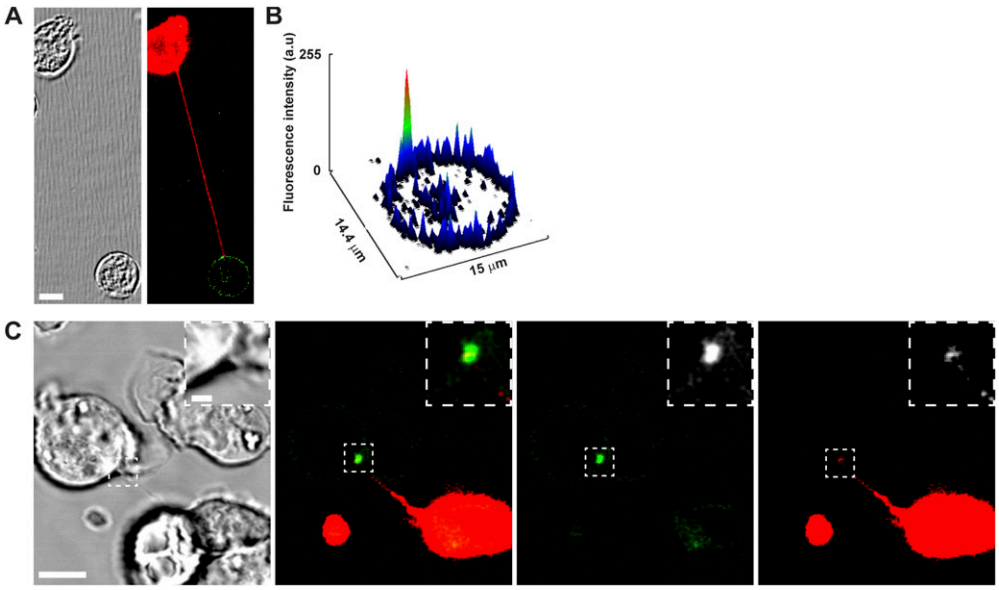

Fig. S5. Accumulation of MICA at NK cell nanotube junction. (*A*) Representative single optical slice shows a single nanotube connecting NKL (labeled with DiD, red) and P815/MICA-YFP (green). (*B*) Intensity of YFP fluorescence around the target cell perimeter shown in *A* has been plotted to reveal a particularly striking accumulation of MICA at the nanotube junction. (*C*) Representative example of MICA accumulation at the nanotube junction formed between primary human NK cells labeled with DiD (red) and P815/MICA-YFP (green, $n > 100$). Boxed regions have been enlarged and gray-scaled to allow better visualization of the accumulation of MICA-YFP. [Scale bars: 10 μm (inserts: 2 μm).]

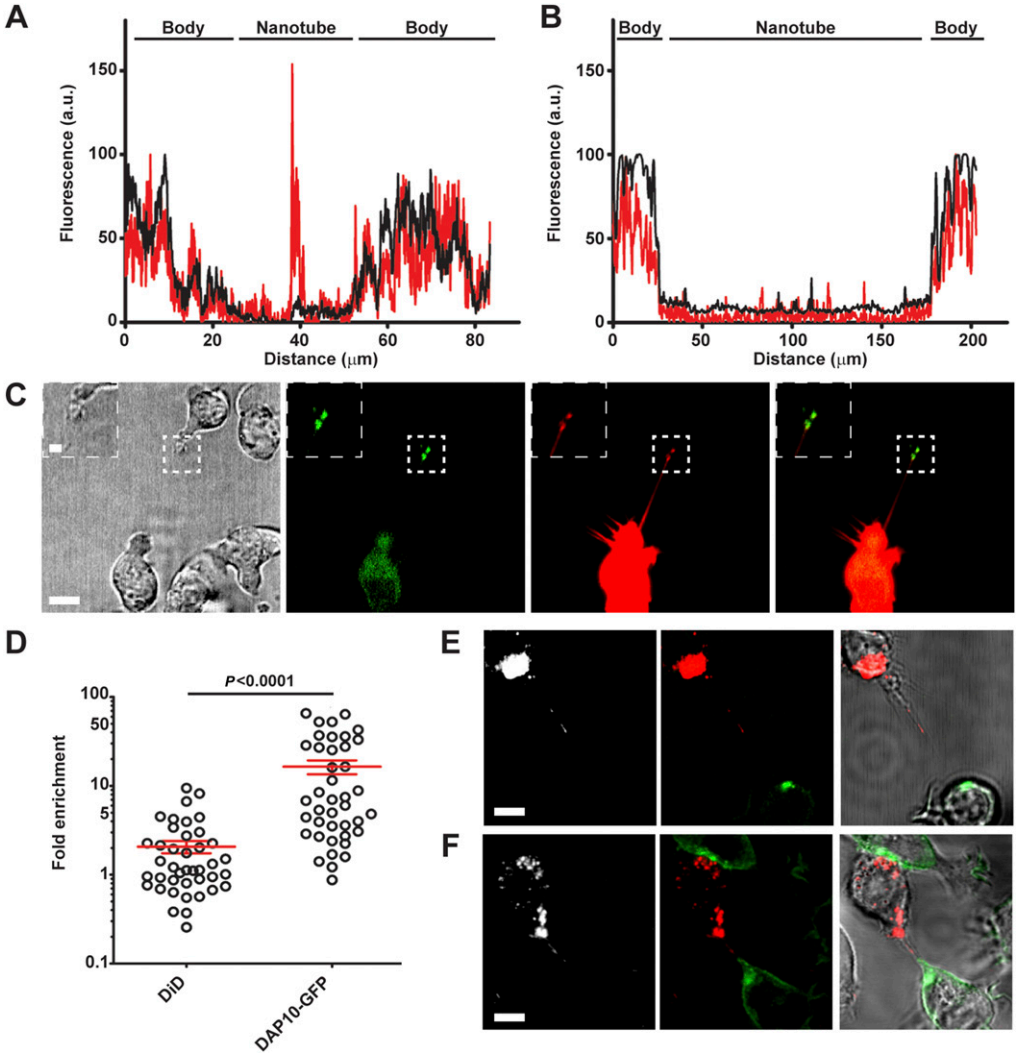

Fig. S6. Signaling can occur at nanotube junctions. (*A* and *B*) Fluorescence intensity traced along the surface of a representative individual cell, including the cell body and nanotube (within an optical section). Fluorescence intensity of DAP10-GFP (*A*) or mem-YFP (*B*) (red lines) with the fluorescence intensity of membrane dye DiD (black lines) is compared for an individual NKL transfectant connected to THP-1 via a nanotube. (*C*) Representative micrograph (n = 41) shows NKL/DAP10-GFP (green) labeled with membrane dye DiD (red), connected to P815/MICA via a nanotube. (*D*) Using NKL/DAP10-GFP and P815/MICA, the fold increase at nanotube junctions of DAP10-GFP and DiD was measured in comparison with that elsewhere along the nanotube. Primary NK cells (*E*) or NKL (*F*) coincubated with 221/MICA-YFP were fixed and stained for perforin (red, n = 20 and n = 10, respectively). [Scale bars: 10 μm (inserts: 2 μm).]

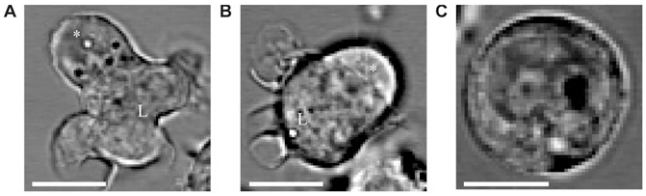

Fig. S7. Determination of cell polarity. (*A* and *B*) Two representative micrographs show examples of polarized P815/MICA-YFP (asterisk marks the uropod and L marks the leading edge). (*C*) Representative example of unpolarized P815/MICA-YFP. (Scale bars: 10 μm.)

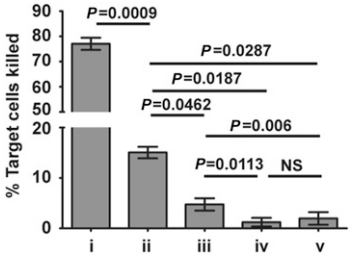

Fig. S8. Relative frequency of different processes leading to target cell death. The relative frequency of different processes that led to death of Daudi/MICA target cells was assessed by analysis of a series of 2-h long movies (n = 235 cell deaths recorded over three independent experiments). Events were scored as death (detected by DNA dye incorporation) occurring (*i*) at a tight cell/cell contact (i.e., via a conventional immune synapse), (*ii*) when target cells were connected to NK cells by nanotubes and had moved back to reform a tight contact, (*iii*) when target cells were connected to a distant NK cell via a membrane nanotube, (*iv*) when target cells had previously been in contact with an NK cell and subsequently moved apart without remaining connected by a nanotube, or (v) when cells spontaneously died without interaction with an NK cell.

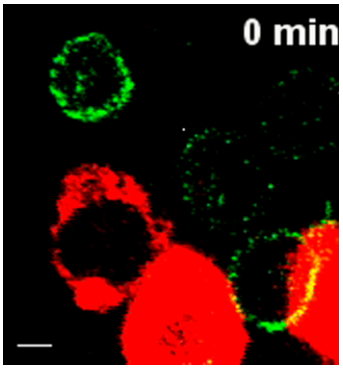

Movie S1. Time-lapse microscopy reveals the formation of nanotubes between NKL and P815/MICA-YFP.

Movie S1

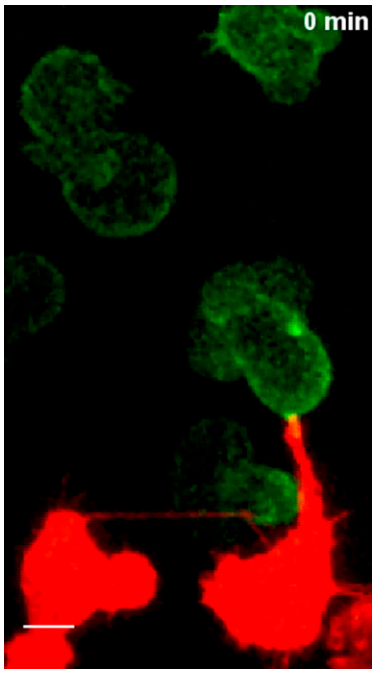

Movie S2. MICA-YFP accumulation is clearly seen at the junction between DiD-labeled NKL (red) and P815/MICA-YFP (green) and is maintained for at least 1 h.

Movie S2

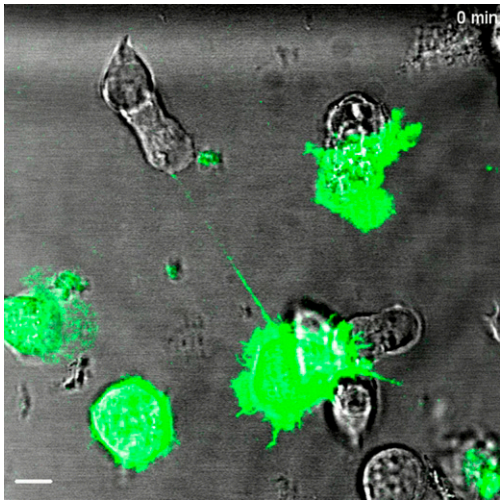

Movie S3. P815/MICA cells can rapidly move back along the nanotube path to form a large contact with NKL/mem-YFP (green).

Movie S3

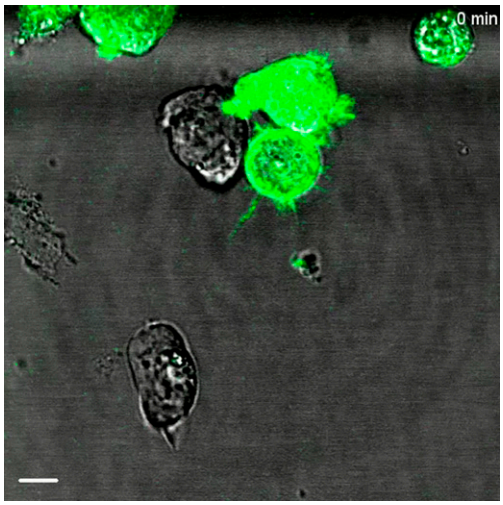

Movie S4. Another example of P815/MICA that rapidly moves back along the nanotube path to form a large contact with NKL/mem-YFP (green).

Movie S4

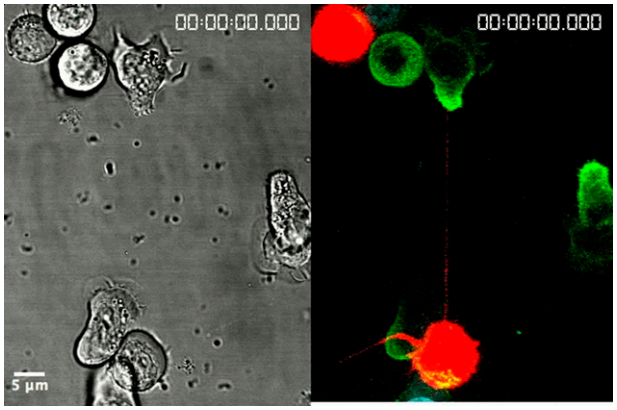

Movie S5. NKL coincubated with 221/MICA-YFP in the presence of a DNA dye, Sytox-blue, which becomes integrated in the nucleus of dying cells following the destruction of the nuclear membrane integrity.

Movie S5

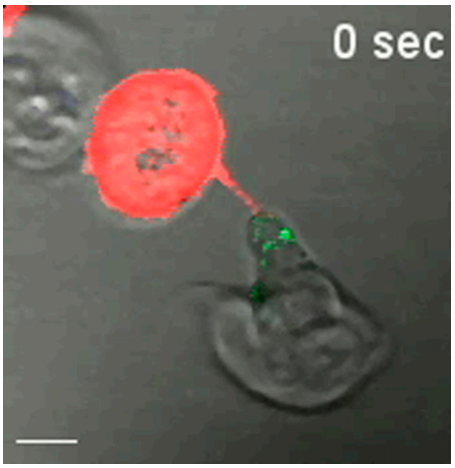

Movie S6. An example of how a nanotube was removed by moving the DiD-labeled (red) NK cell away from a 221/MICA-YFP target cell using a 7-μm needle (red because of autofluorescence) until the nanotube broke.

Movie S6

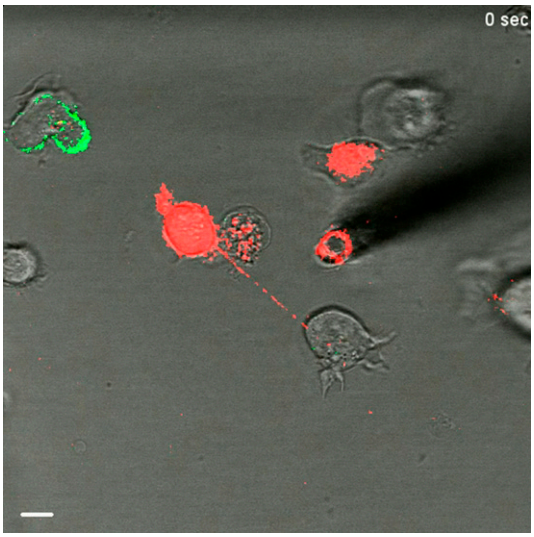

Movie S7. Example of how nanotubes were removed by poking the nanotube connecting DiD-labeled (red) NKL and 221/MICA-YFP (green) using a 7-μm needle (red because of autofluorescence).

Movie S7